

NASA Technical Memorandum 86001

(NASA-TM-86001) HYGROTHERMAL EFFECTS ON
MECHANICAL BEHAVIOR OF GRAPHITE/EPOXY
LAMINATES BEYOND INITIAL FAILURE (NASA)
18 p HC A02/BF A01

N84-32438

CSSL 11D

Unclass

G3/24

23842

Hygrothermal Effects on Mechanical Behavior of Graphite/Epoxy Laminates Beyond Initial Failure

Ori Ishai, Amar Garg, and Howard G. Nelson

August 1984



NASA

National Aeronautics and
Space Administration

Hygrothermal Effects on Mechanical Behavior of Graphite/Epoxy Laminates Beyond Initial Failure

Ori Ishai
Amar Garg
Howard G. Nelson, Ames Research Center, Moffett Field, California



National Aeronautics and
Space Administration

Ames Research Center
Moffett Field, California 94035

HYGROTHERMAL EFFECTS ON MECHANICAL BEHAVIOR OF GRAPHITE/EPOXY LAMINATES BEYOND INITIAL FAILURE

Ori Ishai, Amar Garg, and Howard G. Nelson

NASA Ames Research Center, Moffett Field, California 94035, USA

Abstract

An investigation was conducted to determine the critical load levels and associated cracking beyond which a multidirectional laminate can be considered as structurally failed. Graphite/epoxy laminates were loaded to different strain levels up to ultimate failure. Transverse matrix cracking was monitored by acoustic and optical methods. Residual stiffness and strength that were parallel and perpendicular to the cracks were determined and related to the environmental/loading history. Results indicate that cracking density in the transverse layers has no major effect on laminate residual properties as long as the angle-ply layers retain their structural integrity. Exposure to hot water revealed that cracking had only a small effect on absorption and reduced swelling when these specimens were compared with uncracked specimens. Cracked, moist specimens showed a moderate reduction in strength when compared with their uncracked counterparts. Within the range of environmental/loading conditions of the present study, it is concluded that the transverse cracking process is not crucial in its effect on the structural performance of multidirectional composite laminates.

I. Introduction

Failure of fiber-reinforced plastic laminates is a slow and lengthy process. Transverse cracks are initiated at low loading levels in the first vulnerable plies and continue to accumulate under increased loading conditions up to a saturation crack density.¹⁻⁵ In most structural multidirectional laminates, transverse cracking below the saturation point only slightly affects the global mechanical behavior of the laminate, and no significant reduction in residual stiffness or strength is detected. At saturation crack density, the ply can no longer transfer stresses that are transverse to the fiber direction, and the failed lamina retains only its longitudinal properties and its interlaminar bonding to the neighboring layers. Even at this level of damage, it has been demon-

strated⁶⁻¹⁰ that the global laminate properties are reduced by less than 20%.

Transverse cracks may, however, affect other behavior such as moisture absorption, compressive strength, delamination, and fatigue life. Enhanced moisture absorption in transverse cracked laminates can reduce the durability of the laminate and influence its dimensional stability under prolonged and severe hygrothermal conditions.¹¹ Transverse cracks can reduce the matrix-dominated compressive strength of a laminate. High-stress concentrations caused by the presence of transverse cracks can enhance edge^{10,12,13} and local delamination.¹²⁻¹⁴ Transverse cracking can also influence fatigue life of a laminate.^{4,15}

Most of the previous experimental and analytical work on the influence of transverse cracking has been concerned with the initiation and propagation of transverse cracks and their effect on delamination behavior.²⁻⁸ Much less data and analyses are available on the mechanical post-cracking behavior of the transverse cracked laminates. The objective of the present research is to fill this gap by treating a cracked laminate as a functioning structural element and by providing information about the potential residual structural performance of the damaged composite as it is affected by hygrothermal conditions. The properties that are investigated include stiffness and compressive and flexure strength. The results of this study may extend the usable strength range and raise allowable loading limits above the widely used conservative first-ply-failure limit.

II. Procedure

Research Methodology

The investigation into the residual mechanical behavior of multidirectional graphite/epoxy laminates beyond initial first-ply failure was accomplished in three parts: 1) the controlled introduction of transverse cracks, 2) the hygrothermal conditioning of the damage specimens, and 3) the characterization of residual mechanical behavior (stiffness and strength). The specific details of

the testing program are illustrated in the flow chart shown in Fig. 1.

Material Selection

Based upon a preliminary investigation, it was concluded that in most multidirectional structural laminates, transverse cracking is the predominant initial failure mode. In most cases this failure mode will control the behavior of the laminate at the higher stress levels near ultimate fracture. And, as has been established, transverse cracking is mainly controlled by matrix and fiber-matrix interfacial characteristics. Hence, two material systems were selected which have the same fibers but which have two fundamentally different matrices: 1) T300/934—high-glass transition temperature (T_g), predominantly brittle, high durability, and curing temperature (T_c) of 175°C and 2) T300/5209—relatively low T_g , predominantly ductile, low durability, and T_c of 125°.

Test Specimens

To facilitate direct visible detection of the initial transverse cracks, test specimens were designed to have a 90° ply at the external surfaces. Two types of symmetrical laminate configurations were used: tridirectional [(90/±45/90)_{2S}] and quasi-isotropic [(90/±45/0)_{2S}]. Additionally, reference unidirectional laminates were used for characterization of the basic lamina properties.

Different specimen configurations were used for various testing tasks and loading modes as shown in Table 1. The following was the sequence of specimen testing.

- 1) Specimens were initially loaded in tension to induce transverse cracks.
- 2) The cracked specimens, as well as virgin plates, were cut to smaller specimens and given the desired hygrothermal exposure.
- 3) Dry and wet specimens were cut into smaller specimens that were both parallel and perpendicular to the transverse cracks, and their residual properties were characterized.

Test Procedure

All specimens were vacuum dried at 70°C for a period of not less than 3 weeks prior to the start of the testing procedure.

Introduction of transverse cracks. To establish the relationship between the introduction of transverse cracks and applied strain in the 90° lamina, specimens of the a-4 and a-5 types (Table 1) were loaded in tension. It was found that tensile loading led to a complex cracking pattern, especially during the initial stage of cracking. This was mainly due to the nonuniform cracking process which occurs simultaneously in all 90° layers.

To characterize the transverse cracking process better, type a-6 specimens (Table 1) were tested in flexure. Because only a single 90° lamina at the external specimen surface was exposed to a maximum tensile strain along a relatively small gage length, under this loading condition the transverse cracking process was found to be easily controlled and characterized. In this way, the cracking process and pattern could be isolated and monitored by visual inspection and by acoustic emission (AE) at least during initial stages of loading. The AE total counts and the root mean square (rms) of the AE wave were continuously recorded during the cracking process. The mechanical-acoustic test setups for tension and flexure have been described elsewhere.¹⁶

Based upon the above tests, two transition points in the cracking behavior were identified in terms of the stress-strain relationship and are shown in Fig. 2. The onset of the transverse cracking process was found to occur within a strain range of 0.55% to 0.65%, depending upon the particular material system. First failure of the ±45° plies was found to occur at a strain range of 0.8% to 0.9% and was found to be associated with a change in slope or a knee in the stress-strain curve (Fig. 2).

Micrographs taken from specimens loaded below and above the knee in the stress-strain curve (Fig. 2), before and after transverse cracking of the ±45° plies, are shown in Fig. 3. As can be seen, transverse cracks in the ±45° plies appear to initiate from transverse cracks in the neighboring 90° plies. A similar observation has been reported previously.¹⁷

Specimens that were strained close to ultimate failure were inspected using ultrasonic and x-ray techniques. Previously reported findings of internal delamination^{7,8} and localized delamination

ORIGINAL PAGE IS OF POOR QUALITY

at the root of the transverse cracks¹⁻⁵ were not observed in this study.

Based upon the above observations, transverse cracks were introduced into type a-3 plate specimens (Table 1) of the T300/934, (90/±45/90)_{2S} laminate and the T300/5209, (90/±45/90)_{2S} and (90/±45/0)_{2S} laminates. Selected strain levels of 0.8% and 1.1% (below and above the knee in the stress strain curve, Fig. 2) corresponded to a low level of cracking in the 90° plies and corresponded to a high level of cracking in both the 90° and 45° plies, respectively. These levels correspond to the T300/5209, (90/±45/90)_{2S} system. Plate specimens were loaded in tension to one of these two strain levels and then immediately unloaded.

Hygrothermal conditioning. Cracked and non-cracked "virgin" plates were cut into square specimens (type b-2, Table 1). Some of the specimens were vacuum dried at 70°C and others were immersed in either 70°C water or 40°C water for up to 140 days. Cracked and virgin narrow specimens (types a-6 and b-1, Table 1) were also exposed to similar environmental conditions.

During moisture conditioning, frequent measurements were made of specimen weight and dimensions (along the two major directions) to establish the absorption and swelling characteristics of the cracked and virgin specimens. All measurements were made at room temperature after the specimens were wiped dry. Measurements were made daily during the first week of exposure, and twice a week thereafter. Accuracy of measurement is estimated to be approximately 1 mg in weight and 0.01 mm in length.

When the moisture content of a specimen reached either an intermediate level (approximately 1.0%) or close to saturation (ranging from 1.5% to 2.7% depending on the material system and extent of damage), specimens were stored in 23° water for up to 5 days before mechanical testing. Insignificant change in moisture absorption occurred during this holding period.

Residual property characterization. Wet and dry, cracked, and virgin specimens of types b-2, a-6, and b-1 (Table 1) were cut into specimens of type c (Table 1). The long axis of the specimens were made either perpendicular or parallel to the transverse cracks. Different loading modes were chosen to establish stiffness and compressive and

flexural strength characteristics as shown in Table 1.

Specimens tested under uniaxial loading were tabbed and loaded using a servo-controlled, hydraulic test machine under conditions of a constant displacement rate of approximately 0.025 mm/sec. This displacement rate corresponds to an effective strain rate of approximately 10^{-6} sec⁻¹. In flexure the constant displacement rate was 0.042 mm/sec which corresponds to a maximum strain rate at the external specimen surface of approximately 10^{-6} sec⁻¹.

Special specimen tabs were used because of the high strength and respective loads that are involved in compression testing when the load is parallel to the transverse cracks (and fibers). All compression tests were performed using a wedge-type fixture as recommended by ASTM D-3410.

III. Results and Discussion

The strain required to initiate the first transverse cracks in the outer 90° ply in a tension test are summarized in Table 2. For dry specimens, this strain ranged from 0.5% to 0.65% with the tendency for 5209-epoxy matrix laminates to fall in the upper end of this range. This result is as would be expected; initial transverse cracking is a matrix, and a matrix-interface dominated process, and the 5209 matrix is more ductile than the 934 epoxy matrix. The addition of 1% moisture is seen to substantially increase the strain for first crack initiation in the 934-resin matrix laminate, but it has little effect on the 5209-matrix laminate. Again, these results agree well with laminate analysis which predicts that absorbed moisture can reduce the transverse residual stresses that are built up during post-curing cooling.

Table 2 also summarizes the observed strain for the initiation of ±45° ply failure (knee in the stress-strain curve, Fig. 2) and for ultimate laminate failure. The strains for these two critical stages of failure appear relatively independent of both matrix and specific laminate lay-up.

The experimental results shown in Table 2 were compared with analytical computations based on a modification of the classical laminate theory. In this analysis, the effects of the cracked layers on

ORIGINAL PAGE IS
OF POOR QUALITY

laminates were evaluated by replacing these layers in the model with those that retain only the longitudinal properties of the original plies. In most cases this analysis gave good agreement with the experimentally observed results.

Based upon the cracking patterns observed by the use of the replicating tape technique during multistage loading, several quantitative relationships can be developed. As shown in Fig. 4, crack density in the outer 90° ply was found initially to increase linearly with increased flexural strain. At high-strain levels, as ultimate failure is approached, the rate of cracking is reduced significantly and the crack density appears to approach saturation.

Moisture was found to significantly influence the general cracking process and the associated cracking pattern. In dry specimens, continuous and straight transverse cracks were present across the specimen width from one edge to the other. This suggests that transverse crack growth in these specimens is a continuous and spontaneous process once the crack has been initiated. In wet specimens, several cracks appear to arrest within the lamina. Typical cracking patterns observed for a given strain in the dry and the wet specimens are shown in Fig. 5. These observations are again in agreement with the idea that moisture increases the plasticity of the resin matrix.

As reported previously,¹⁶ acoustic emission appears to be a reliable technique for the detection and monitoring of the cracking process. As shown in Fig. 6 for the T300/934 laminate, the total AE count was found to vary linearly with crack density at the lower crack densities. Additionally, little or no difference was observed between wet and dry specimens in this region. At high-crack densities the wet specimen remained linear whereas a sharp increase in total count was observed in the dry specimen. This latter observation suggests that the initiation of an additional source of noise exists above that which results from outer ply transverse cracking. This source of noise appears to be the initiation and propagation of transverse cracks in the inner plies. Again, moisture enhances the ductility of the resin matrix and delays the occurrence of transverse cracking in the inner plies.

Moisture absorption and swelling were studied in unidirectional laminates of T300/934 and of T300/5209 in order to establish a base for the evaluation of hygrothermal effects in virgin and damaged multidirectional laminates. The typical time dependence of moisture absorption observed in unidirectional laminates is shown in Fig. 7. As would be expected, laminate thickness was found to influence the rate of moisture absorption, but the width of the laminate had no effect. Saturation moisture level was independent of both laminate thickness and width. The moisture saturation levels observed for the unidirectional laminates are listed in Table 3.

Moisture absorption versus time behavior of typical multidirectional laminates is shown in Fig. 8 for both virgin and cracked specimens. In the T300/934 system that is exposed to 70°C water, the cracked laminate is characterized by a higher absorption rate when it is compared with its virgin reference. For the T300/5209 system, however, transverse cracking was found to have no effect upon the rate of moisture absorption at 70°C. One possible explanation for this latter behavior is that 70°C is close to the T_g of the 5209 matrix material and moisture absorption is inherently rapid at these temperatures. On the other hand, when the T300/5209 laminate was exposed to 10°C water, the cracked specimens exhibited a significantly higher absorption rate than the virgin references did in much the same manner as that presented in Fig. 8 (see Table 3).

The relationship between swelling and moisture content for T300/934 unidirectional laminates exposed to 70°C water is shown in Fig. 9. After an initial transient up to approximately 0.6% moisture, transverse swelling is linearly dependent upon moisture content. Additionally, swelling strains versus moisture content relationship appear independent of laminate thickness.

Similarly, the typical relationship between swelling strain and moisture content observed for the (90/±45/90)_{2S} multidirectional laminates is shown in Fig. 10. As would be expected, transverse swelling is much less for this multidirectional laminate than for the unidirectional laminate (Fig. 9) and data scatter is much greater. In fact, moisture-induced swelling in the (90/±45/0)_{2S}

ORIGINAL QUALITY OF POOR QUALITY

laminates was below the resolution of the measuring system. As can be seen in Fig. 10, after an initial transient up to approximately 0.6% moisture, swelling appears linearly dependent upon moisture level. The damaged laminate exhibits less swelling for a given moisture content than it does for the uncracked, virgin laminate.

The slope of the linear portion of the swelling curve is defined as the hydroelastic coefficient, β_x . A summary of the β_x values observed for all the laminates that are investigated is given in Table 3. As can be seen, because of the lack of constraint in the transverse direction, β_x in unidirectional laminates is much greater than in multidirectional laminates. Multidirectional laminates of the T300/934 system exhibit a much greater β_x than those of the T300/5209 system do when exposed to 70°C water. (Input data for analysis of T300/5209 laminates were taken from Ref. 18. It indicates significantly low transverse and shear moduli for this system at this temperature level, which is close to the T_g of its matrix.) In all cases, damaged laminates are seen to exhibit a lower value of β_x than their virgin counterparts. This trend agrees well with analytical results, based on the modified laminate theory, as shown in Table 4. The trend is attributable to the decrease in stiffness of the cracked 90° layers which then reduces the swelling effect of these layers on the whole multidirectional laminate.

Residual stiffness and strength characteristics of multidirectional laminates that contained various crack densities were determined. Residual stiffness in tension and flexure were established using multicycle loading where the initial tangent modulus was measured and related to the maximum strain of the preceding cycle (ϵ_L). Figure 11 shows the observed strain dependence of the normalized residual tangent modulus [modulus of the cracked laminate divided by the initial modulus of the respective virgin (uncracked) laminate] for the T300/5209, (90/±45/90)_{2S} laminate. From the previously established relationship between transverse crack density and applied strain (Fig. 4), the relationship between the normalized tangent modulus and the transverse crack density can be established and is shown in Fig. 12. As can be seen from this figure, stiffness begins to decay only after a significant amount of transverse

cracking has occurred. Even at this point, the degradation in stiffness in the cracked laminate is only about 10% of that of the virgin laminate at a crack density of approximately 5 cracks/cm. Similar reductions were observed for the T300/934, (90/±45/90)_{2S} laminate. All data are summarized in Table 4.

Also shown in Table 4 are results of the quasi-isotropic laminate (90/±45/0)_{2S}. As can be seen, the reduction in residual stiffness for this laminate is essentially negligible even at a high-crack density. This is what would be expected since the transverse layers in the laminate contribute little to its overall stiffness. Moisture seems to have an insignificant effect on elastic moduli of both cracked and virgin specimens. Analytical results based on the modified laminate theory predict higher deterioration in residual stiffness of cracked specimens as compared with experimental data (Table 4).

Table 5 summarizes the results of residual compressive strength tests that were performed on the multidirectional laminate, cracked and uncracked, and dry and wet. In the cracked specimens, load was either applied along the cracking direction or perpendicular to the transverse cracks. Failure always occurred in the free gage length by a "buckling-delamination" type failure mode as shown in Fig. 13.

As can be seen in Table 5, the presence of transverse cracks, even at a high-crack density, does not have a significant effect on the residual compressive strength of either material system, multidirectional laminate, or moisture condition investigated. In almost all cases, residual compressive strength was greater than 90% of that of the uncracked, virgin specimens. In general, wet specimens are seen to have a lower compressive strength than do dry specimens. Oddly enough, in some cases cracking of the transverse ply in combination with moisture appears to increase the residual strength characteristics. This is most probably a result of both the release of the inherent residual stresses in the laminate and the increased ductility of the epoxy matrix that are induced by the presence of moisture.

Similar results were observed for residual flexure strength and are summarized in Table 6.

Residual flexure strength of cracked specimens was in no case less than 90% of the virgin references; in some cases strength was unaffected by the presence of either transverse cracking or moisture.

IV. Conclusions

Multidirectional T300/5209 and T300/934 laminates were studied in an effort to establish the effect of transverse cracks on their residual mechanical behavior when exposed to selected hydrothermal conditions. The introduction of transverse cracks was found to vary linearly with applied strain (after some initial strain) and to approach a saturation crack density. Moisture was found to delay the onset of transverse cracking and to slow down crack propagation.

The presence of transverse cracks was found to slightly enhance moisture absorption into the laminates at lower temperatures, but it had a negligible effect at high temperatures that approached the T_g of the matrix. Moisture-induced expansion of the laminates was found to be less for cracked laminates when they were compared with virgin, uncracked laminates.

Transverse cracks, even at levels that approached saturation crack density, were found to reduce the stiffness and compressive and flexural strengths of the multidirectional laminates by less than 10%. Hygrothermal conditions had little influence on these effects and, in almost all cases, the residual properties of the crack laminates were greater than 90% of that of the uncracked, virgin laminates. Based on present results, which are limited to quasi-static loading and moderate hygrothermal conditions, it is concluded that matrix transverse cracking is not a crucial process in affecting the structural performance of multidirectional composite laminates.

References

¹Ishai, O. and Lavengood, R., "The Mechanical Performance of Bidirectional Fiber-glass Polymeric Composites," *Israel Journal of Technology*, Vol. 8, No. 1-2, 1970, pp. 101-109.

²Highsmith, A. L. and Reifsnider, K. L., "Stiffness-reduction Mechanism in Composite Laminate," *ASTM Symposium on Damage in Composite Materials*, ASTM STP-775, 1980, pp. 103-107.

³Masters, E. and Reifsnider, K. L., "An Investigation of Cumulative Damage Development in Quasi-isotropic Graphite/Epoxy Laminates," *ASTM Symposium on Damage in Composite Materials*, ASTM STP-775, 1980, pp. 40-61.

⁴Reifsnider, K. L. and Jamison, R., "Fracture of Fatigue-loaded Composite Laminates," *Int. J. of Fatigue*, 1982, pp. 187-198.

⁵Reifsnider, K. L., Henneke, E. G., Stinchcomb, W. W., and Duke, J. C., "Damage Mechanics and NDE of Composite Laminates," *Proceedings of IUTAM Symposium on Mechanics of Composite Materials*, Pergamon Press, 1983, pp. 399-420.

⁶Nuismer, R. J. and Tan, S. C., "The Role of Matrix Cracking in the Continuum Constitutive Behavior of a Damaged Composite Ply," *Proceedings of the IUTAM Symposium on Mechanics of Composite Materials*, 1982, pp. 437-448.

⁷Crossman, F. W., Warren, W. J., Wang, A. S. D., and Law, G. E., "Initiation and Growth of Transverse Cracks and Edge Delamination in Composite Materials," *J. of Composite Materials*, Vol. 14, 1980, pp. 88-108.

⁸Crossman, F. W. and Wang, A. S. D., "The Dependence of Transverse Cracking and Delamination on Ply Thickness in Graphite/Epoxy Laminates," *ASTM Symposium on Damage in Composite Materials*, ASTM STP-775, 1980, pp. 118-139.

⁹O'Brien, T. K., Ryder, J. T., Canyon, R., and Crossman, F. W., "Stiffness, Strength, Fatigue Life Relationships for Composite Materials," *AFWAL-TR-82-4007*, 1982, pp. 79-90.

¹⁰Wang, A. S. D. and Crossman, F. W., "Fracture Growth in Composite Laminates," *AFWAL-TR-82-4007*, 1982, pp. 91-104.

¹¹Eselun, S. A., Neubert, H. D., and Wolf, E. G., "Microcracking Effects on Dimensional Stability," *Proceedings of the 24th National Society for the Advancement of Material and Process Engineering (SAMPE) Symposium*, 1979, pp. 1299-1309.

¹²O'Brien, T. K., "Characterization of Delamination Onset and Growth in a Composite Laminate," *ASTM STP-775*, 1982, pp. 140-167.

¹³O'Brien, T. K., "Mixed-mode Strain-energy Rate Effects on Edge Delamination of Composites," *NASA TM-84592*, 1983.

¹⁴Kim, R. Y., "A Technique for Prevention of Delamination," AFWAL-TR-82-4007, 1982, pp. 218-230.


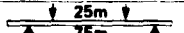




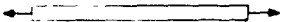


¹⁵Jamison, R. D., Schulte, K., Reifsnider, K. L., and Stinchcomb, W. W., "Characterization and Analysis of Damage Mechanism in Fatigue of Graphite/Epoxy Laminates," ASTM Symposium on Effect of Defects in Composite Materials, Dec. 1982.

¹⁶Garg, A. and Ishai, O., "Characterization of Delamination and Transverse Cracking in Graphite/Epoxy Laminates by Acoustic Emission," 1st International Symposium on Acoustic Emission from Reinforced Composites, July 1983. (Also NASA TM-84370, 1983.)

¹⁷Kim, R. Y. and Aoki, R. M., "Transverse Cracking and Delamination in Composite Materials," Fiber Science and Technology, Vol. 18, 1983, pp. 203-216.

¹⁸Crossman, W., Mauri, R. T., and Warren, W. J., "Hygrothermal Damage Mechanisms in Graphite/Epoxy Composites," Nasa CR-3189, 1979.

Table 1 Specimen geometries and testing tasks.

TEST OBJECTIVE	LOADING MODE	ILLUSTRATION OF SPECIMEN IN TEST	SPECIMEN DIMENSION (mm)	SPECIMEN I. D
BASIC MECHANICAL PROPERTIES	TENSION		250 x 12	a - 1
" " "	4 POINT FLEXURE		100 x 12	a - 2
INDUCING TRANSVERSE CRACKING	TENSION		270 x 64	a - 3
			250 x 12	a - 4
			250 x 18	a - 5
" " "	4 POINT FLEXURE		100 x 18	a - 6
HYGROTHERMAL CHARACTERISTICS (ABSORPTION AND SWELLING)			100 x 12	b - 1
			60 x 64	b - 2
RESIDUAL PROPERTIES CHARACTERISTICS	TENSION		250 x 18	c - 1
	3 POINT FLEXURE		64 x 6	c - 2
			64 x 12	c - 3
	COMPRESSION		64 x 6	c - 4

ORIGINAL PAGE IS
OF FOOTNOTES

Table 2 Summary of experimental and analytical results for critical strains and stresses observed during tensile loading of multidirectional graphite/epoxy laminates (see Fig. 2).

Material system	Moisture content, w (%)	Cracking initiation (FCI)		Failure of $\pm 45^\circ$ layer ("knee")		Ultimate laminate failure (ULF)			Loading level of plates		
		Strain, ϵ_{ic} (%)	Stress, σ_{ic} (MPa)	Strain, ϵ_p (%)	Stress, σ_p (MPa)	Strain, ϵ_u (%)	Stress, σ_u (MPa)	Crack density (cracks/cm)		Strain, ϵ_L (%)	Crack density (cracks/cm)
T300/5209 (90/ ± 45 /0) _{2s}	0	Experiment 0.60- -0.65	300 -330	0.84	420	4-5	1.14	560	7-8	0.85	5-6
		Computed 0.50	263	0.69	364		0.97	492			
T300/5209 (90/ ± 45 /90) _{2s}	0	Experiment 0.56- -0.65	124- -144	0.88	188	5-6	1.20	220	7-9	0.80 1.10	3-4 6-7
		Computed 0.57	128	0.75	168						
T300/934 (90/ ± 45 /90) _{2s}	0	Experiment 0.50- -0.55	115- -126	0.76	160	5-6	1.10	200	9-10	0.96	7-8
		Computed 0.49	116	0.74	177						
T300/5209 (90/ ± 45 /90) _{2s}	-1.0	Experiment 0.63	150								
		Computed 0.65	146								
T300/934 (90/ ± 45 /90) _{2s}	-1.0	Experiment 0.70	148								
		Computed 0.68	152								

ORIGINAL PAGE IS
OF POOR QUALITY

Table 3 Experimental data and analytical results for hygrothermal characteristics of different graphite/epoxy laminates.

Material system	Laminate configuration (lay-up)	Environmental conditions	Loading history	Maximum moisture content, v_m (%)	Transition moisture content, w_0 (%)	Hygro-expansion coefficient (HEC), β_x	
						Experiment	Computed
T300/934	(90) ₀ (90) ₁₆	70°C water	Virgin	1.52	0.56	0.56	--
T300/5209	(90) ₁₆	70°C water	Virgin	1.82	0.58	0.55	--
T300/934	(90/±45/90) ₂₈	70°C water	Virgin	1.68	0.58	0.156	0.189
			Cracked, $\epsilon_L = 0.96\%$	1.80	0.58	0.089	0.086
T300/5209	(90/±45/90) ₂₈	70°C water	Virgin	2.31	--	0.049	0.047
			Cracked, $\epsilon_L = 1.1\%$	2.27	--	0.034	0.018
T300/5209	(90/±45/90) ₂₈	40°C water	Virgin	1.19	0.45	0.131	0.138
			Cracked, $\epsilon_L = 1.1\%$	1.49	0.40	0.065	0.059
T300/5209	(90/±45/0) ₂₈	70°C water	Virgin	2.70	--	(a)	0.0093
			Cracked, $\epsilon_L = 0.85\%$	2.64	--	(a)	0.0046

Note: All specimens exposed to hot water for more than 12 weeks.

^aDeformations too small for measurement.

Table 4 Average experimental data versus analytical results for residual elastic modulus of cracked and virgin graphite/epoxy multidirectional laminates.

Material system	Loading mode	Preloading strain, ϵ_L (%)	Experimental results			Analytical results		
			Virgin, E_0	Cracked, E_c	Normalized, E_c/E_0	Virgin, E_0	Cracked, E_c	Normalized, E_c/E_0
T300/934 (90/±45/90) _{2S}	Flexure	0	22.90		0.89	23.76		
		1.7		20.50			18.84	0.79
T300/5209 (90/±45/90) _{2S}	Tension	0	21.70		0.93	22.51		
		1.1		20.10			18.54	0.82
T300/5209 (90/±45/0) _{2S}	Tension	0	51.20		0.98	52.56		
		1.0		50.20			50.72	0.96

Note: E in GPa.

Table 5 Summary of residual compressive strengths for cracked and virgin multidirectional laminates in both the wet and dry conditions.

Material	Test lay-up	Moisture content, w (%)	Loading direction	Loading strain, ϵ_L (%)	Compressive strength, MPa
T300/5209	(0/±45/0) _{2S}	0	Along cracks	0	899
				0.8	833
				1.1	825
T300/5209	(0/±45/90) _{2S}	0	Along cracks	0	595
				0.85	562
T300/934	(0/±45/0) _{2S}	0	Along cracks	0	958
				0.96	930
T300/5209	(90/±45/90) _{2S}	0	Perpendicular to cracks	0	245
				0.8	234
				1.1	227
T300/5209	(90/±45/0) _{2S}	0	Perpendicular to cracks	0	96
				0.85	10
T300/934	(90/±45/90) _{2S}	0	Perpendicular to cracks	0	255
				0.96	239
T300/5209	(0/±45/0) _{2S}	2.35	Along cracks	0	815
				0.8	777
				1.1	709
T300/5209	(0/±45/90) _{2S}	2.83	Along cracks	0	407
				0.85	444
T300/934	(0/±45/0) _{2S}	1.86	Along cracks	0	830
				0.96	805
T300/5209	(90/±45/90) _{2S}	2.53	Perpendicular to cracks	0	197
				0.8	184
				1.1	200
T300/5209	(90/±45/0) _{2S}	2.75	Perpendicular to cracks	0	452
				0.85	450
T300/934	(90/±45/90) _{2S}	1.94	Perpendicular to cracks	0	257
				0.96	262

ORIGINAL PAGE IS
OF POOR QUALITY

ORIGINAL PAGE 19
OF POOR QUALITY

Table 6 Summary of residual flexural strengths for cracked and virgin multidirectional graphite/epoxy laminates in both the wet and dry conditions.

Material	Test lay-up	Moisture content, w (%)	Loading direction	Loading strain, ϵ_L (%)	Compressive strength, MPa
T300/934	(0/±45/0) ₂₈	0	Along cracks	0 0.96	1006 1002
T300/934	(0/±45/0) ₂₈	1.86	Along cracks	0 0.96	978 932
T300/5209	(0/±45/0) ₂₈	2.35	Along cracks	0 0.8 1.1	955 910 907
T300/5209	(0/±45/90) ₂₈	2.82	Along cracks	0 0.85	623 558
T300/934	(90/±45/90) ₂₈	1.55	Perpendicular to cracks	0 0.96	341 342
T300/5209	(90/±45/90) ₂₈	2.53	Perpendicular to cracks	0 0.8 1.1	260 237 247
T300/5209	(90/±45/0) ₂₈	2.82	Perpendicular to cracks	0 0.85	650 630

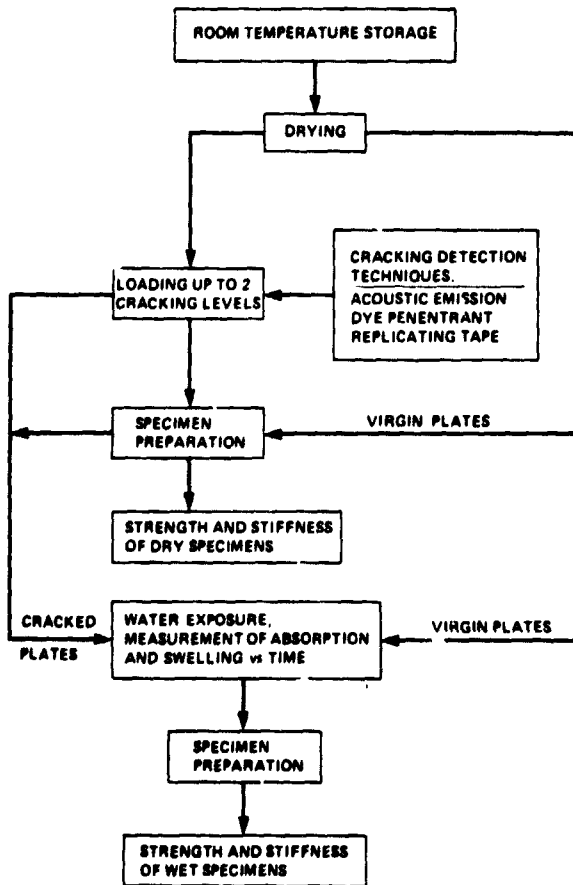


Fig. 1 Testing procedure of graphite/epoxy specimens.

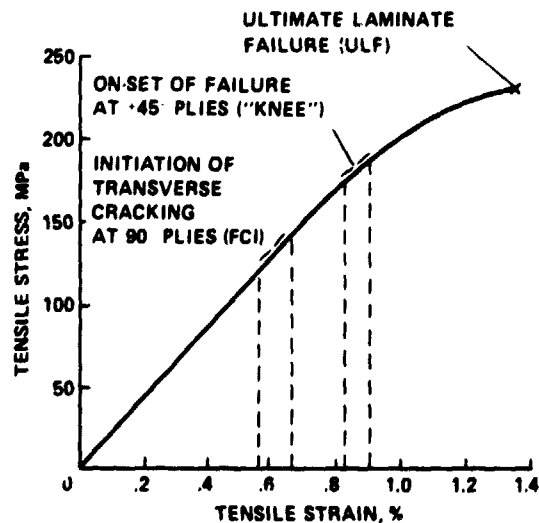


Fig. 2 Typical stress-strain relationship for a (90/±45/90)₂₈ dry graphite/epoxy specimen in tension (see Table 2).

ORIGINAL PAGE IS
OF POOR QUALITY

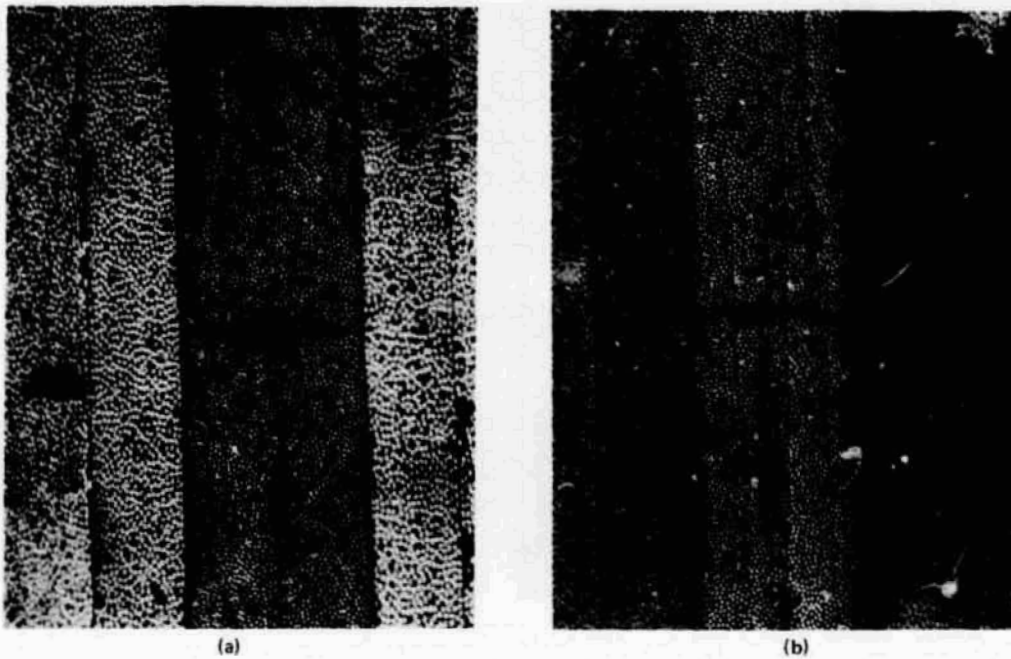


Fig. 3 Micrographs showing typical transverse cracks formed in tension. a) Below "knee" transition; b) above "knee" transition.

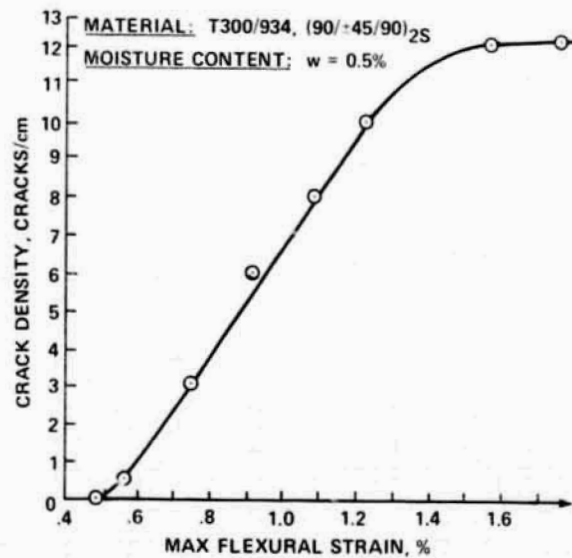


Fig. 4 Typical crack density versus flexural strain relationship for graphite/epoxy specimens loaded in flexure.

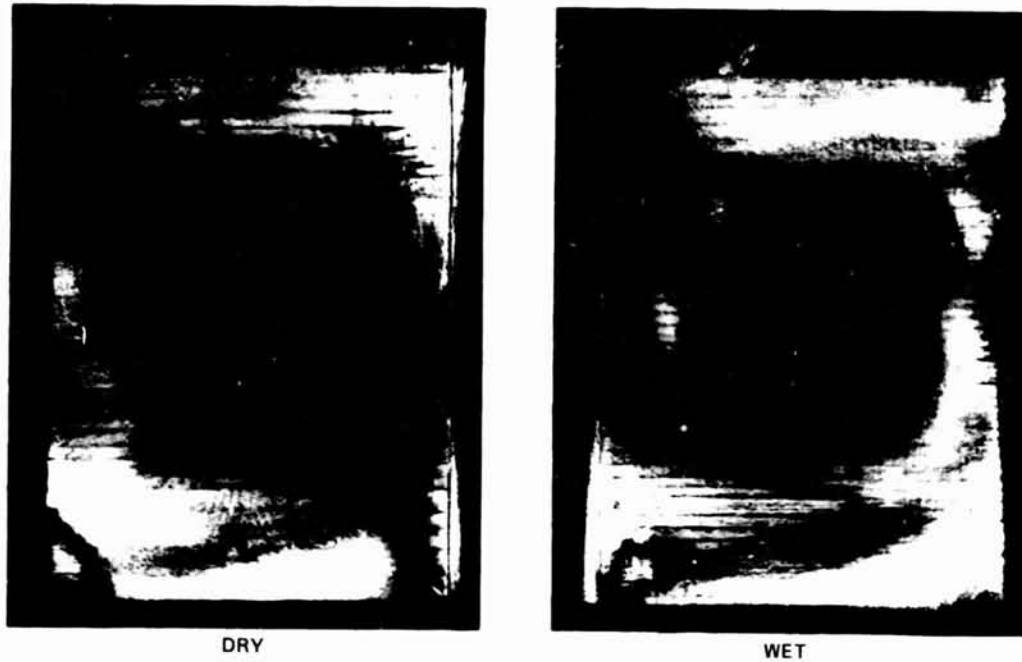


Fig. 5 Typical cracking pattern in dry and wet ($w = 1.0\%$) graphite/epoxy specimens [T300/5209, $(90/\pm 45/90)_{2S}$] loaded in flexure to high-flexural strain level ($\epsilon_L = 1.48\%$) (replicating tape technique magnification: $\times 3$).

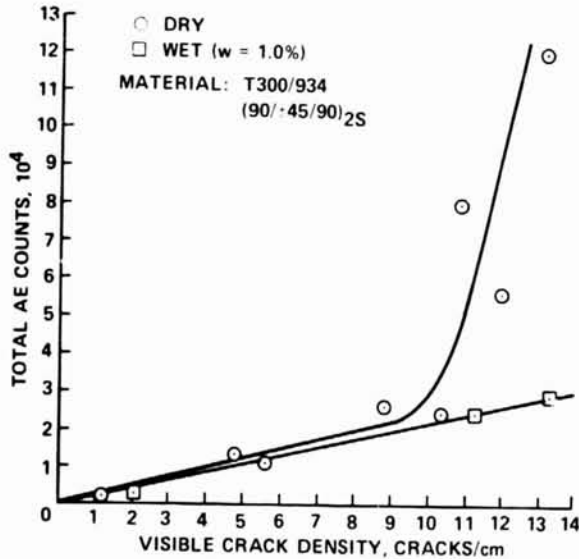


Fig. 6 Total AE counts versus crack density for dry and wet graphite/epoxy specimen loaded in flexure.

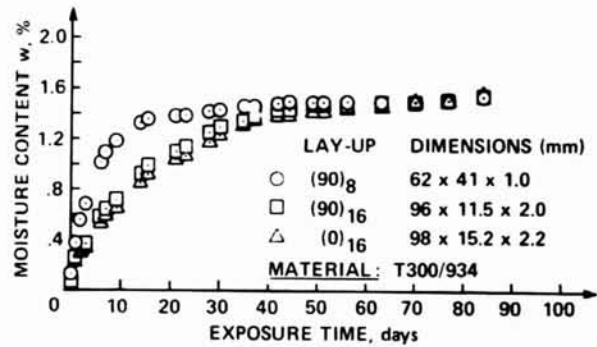


Fig. 7 Moisture absorption behavior of unidirectional graphite/epoxy laminates exposed to 70°C water.

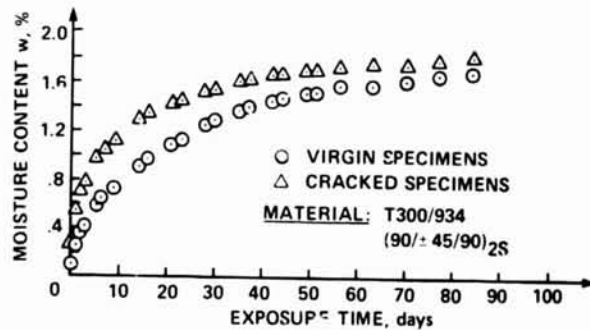


Fig. 8 Moisture absorption behavior of multi-directional graphite/epoxy laminates exposed to 70°C water.

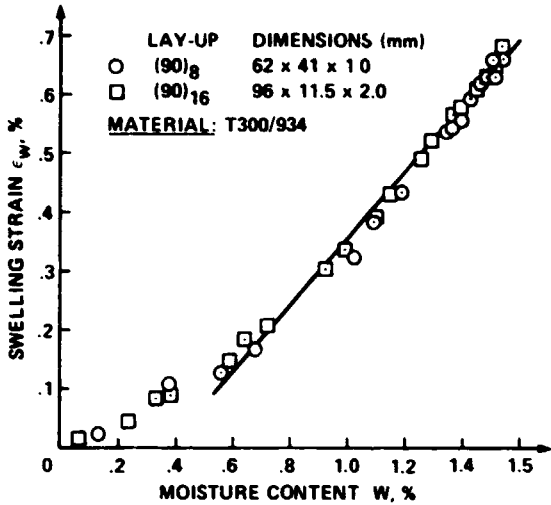


Fig. 9 Swelling versus moisture absorption relationship for unidirectional graphite/epoxy laminates exposed to 70°C water.

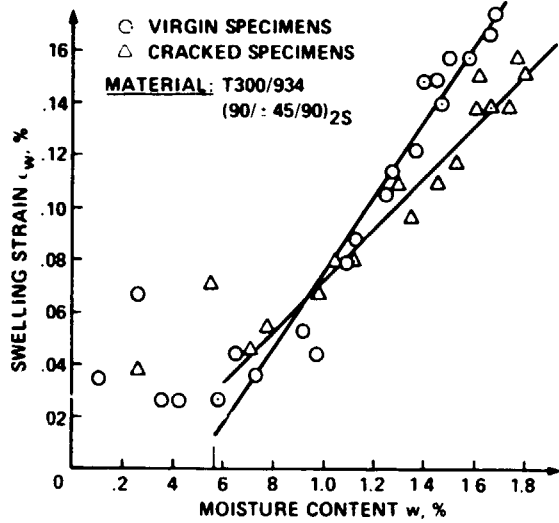


Fig. 10 Swelling versus moisture absorption relationship for multidirectional graphite/epoxy laminates exposed to 70°C water.

ORIGINAL PHOTO
OF POOR QUALITY

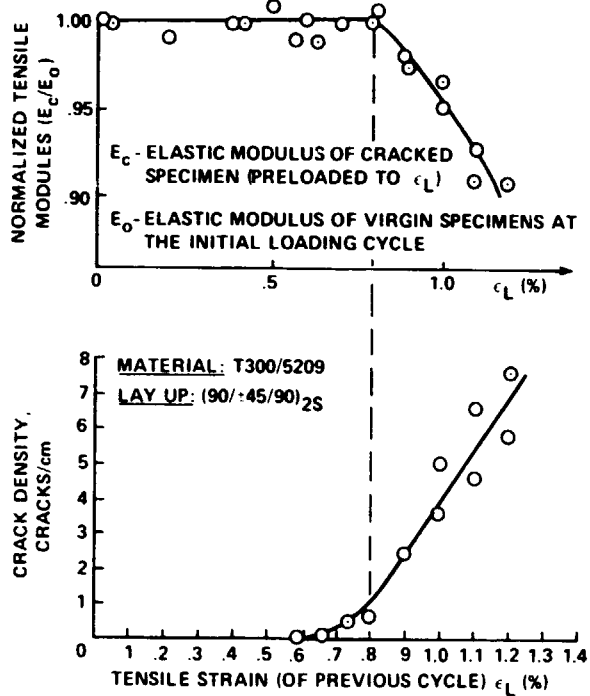


Fig. 11 The effect of preloading tensile strain (ϵ_L) and subsequent cracking on normalized tangent modulus in dry multidirectional graphite/epoxy specimens.

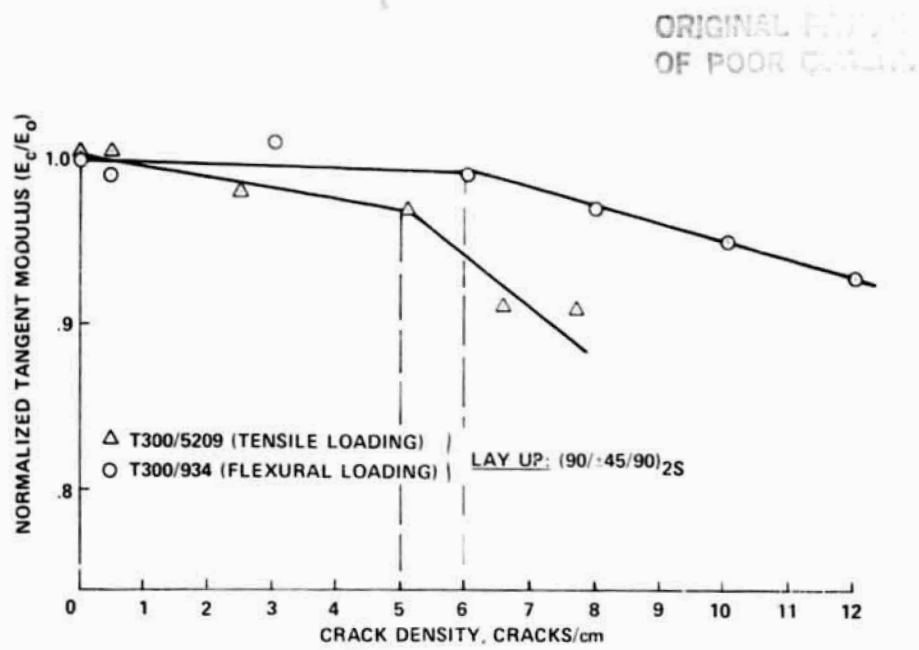


Fig. 12 Residual normalized tangent modulus versus crack density in multidirectional graphite/epoxy specimens.



Fig. 13 Typical compressive-failed specimens loaded parallel (a) and perpendicular (b) to cracking orientation (x7).